Molecular Pharmacology Fast Forward. Published on April 4, 2011 as doi: 10.1124/mol.111.071787

In vivo and in vitro characterization of a first-in-class novel azole analog that targets PXR activation

Madhukumar Venkatesh, Hongwei Wang, Julie Cayer, Melissa Leroux, Dany Salvail, Bhaskar Das, Sridhar Mani

Albert Einstein Cancer Center, Albert Einstein College of Medicine, New York, New York. 10461 (M.V., H.W., B. D., S. M.)

IPS Therapeutique Inc., Sherbrooke, Canada. J1E 4K8 (J.C., M.L., D.S.)

Molecular Pharmacology Fast Forward. Published on April 4, 2011 as DOI: 10.1124/mol.111.071787
This article has not been copyedited and formatted. The final version may differ from this version.

Running title: PXR, azole analogs and drug resistance

Corresponding author: Dr. Sridhar Mani, Albert Einstein College of Medicine, 1300 Morris Park avenue, Chanin 302D-1, New York, New York 10461. Tel: 718-430-2871; Fax: 718-904-2830; Email: sridhar.mani@einstein.yu.edu

The number of text pages-36

Number of tables-3

Number of figures-7

Number of references-48

Number of words in abstract-183

Number of words in Introduction-694

Number of words in results-2010

Number of words in Discussion-949

ABBREVIATIONS: PXR, pregnane X receptor; mCAR, mouse constitutive androstane receptor; LXR, liver X receptor; FXR, farnesoid X receptor; ERα, estrogen receptor alpha; PPARγ; peroxisome proliferator activated receptor gamma; PCN, pregnenolone-16alpha-carbonitrile; APAP, Acetaminophen, Rif, rifampicin; qPCR, quantitative polymerase chain reaction; SSA,serum amyloid A.

Molecular Pharmacology Fast Forward. Published on April 4, 2011 as DOI: 10.1124/mol.111.071787
This article has not been copyedited and formatted. The final version may differ from this version.

Abstract

The pregnane X receptor (PXR) is a master regulator of xenobiotic clearance and is implicated in deleterious drug interactions (e.g., acetaminophen hepatotoxicity) and cancer drug resistance. However, small molecule targeting of this receptor has been difficult and, to date, directed synthesis of a relatively specific PXR inhibitor has remained elusive. Here we report the development and characterization of a first-in-class novel azole analog (compound 3, FLB-12) that antagonizes the activated state of PXR with limited effects on other related nuclear receptors (i.e., LXR, FXR, ERα, PPARγ and mCAR). We investigated the toxicity and PXR antagonist effect of compound 3 *in vivo*. When compared with ketoconazole, a prototypical PXR antagonist, compound 3 is significantly less toxic to hepatocytes. Compound 3 significantly inhibits the PXR-activated loss of righting reflex to avertin *in vivo*, abrogates PXR-mediated resistance to SN-38 in colon cancer cells *in vitro*, and attenuates PXR-mediated acetaminophen hepatotoxicity *in vivo*. Thus, relatively selective targeting of PXR by antagonists is feasible and warrants further investigation. This class of agents is suitable for development as chemical probes of PXR function, as well as potential PXR-directed therapeutics.

Molecular Pharmacology Fast Forward. Published on April 4, 2011 as DOI: 10.1124/mol.111.071787
This article has not been copyedited and formatted. The final version may differ from this version.

Introduction

The pregnane X receptor (PXR) is an adopted orphan nuclear receptor that functions as a classical RXRα heterodimer. It controls gene expression in response to ligands as small as estradiol (268 Da) to large macrolide antibiotics, for example, rifampicin (823 Da). In its role as a xenosensor, PXR regulates the expression of genes in response to potentially toxic endogenous (bile acids) and exogenous chemicals (xenobiotics); however, ligand activated PXR (e.g., St. John's Wort; hyperforin) has been implicated in deleterious drug interactions (e.g., reductions in serum levels of oral contraceptives and chemotherapeutics, such as camptothecins, indinavir and cyclosporine), inconsistent drug bioavailability (e.g., digoxin), exclusion of central nervous system (CNS) acting drugs due to enhanced blood brain barrier transporter expression (e.g., P-gp, MRP2), and resistance to cancer drugs [reviewed in (Biswas et al., 2009)]. Our laboratory has demonstrated that one possible mechanism of PXR mediated drug resistance involves the tumoral induction of cytochrome P450 and transporters (Gupta et al., 2008).

Based on these observations, it is evident that antagonists of PXR could be essential tools to probe PXR biology (e.g., the mechanisms underlying drug interactions mediated by PXR) and, importantly, serve as potential pharmaceuticals for a wide-based application in humans. (e.g., the reversal of drug resistance and enhanced drug delivery) [reviewed in (Biswas et al., 2009)] (Harmsen et al., 2009). PXR is activated by a wide variety of structurally diverse compounds (Kortagere et al., 2010), including many anti-cancer drugs (Harmsen et al., 2009; Raynal et al., 2010). While such as rifampicin are described in the literature, only a few weak PXR antagonists have been reported (e.g., ET-743, A-792611 and sulforaphane) [reviewed in (Biswas et al., 2009)]. Takeshita et al. (Takeshita et al., 2002) originally described ketoconazole as a PXR antagonist, but its exact mechanism was elusive. Our laboratory was the first to report the likely

Molecular Pharmacology Fast Forward. Published on April 4, 2011 as DOI: 10.1124/mol.111.071787
This article has not been copyedited and formatted. The final version may differ from this version.

mechanisms of ketoconazole's action by demonstrating its antagonist effect on the AF-2 PXR co-regulator interaction surface (Ekins et al., 2007; Huang et al., 2007; Wang et al., 2007). Subsequent studies demonstrated that ketoconazole exhibits distinct features pertinent to antagonists (when compared with ligand pocket binding agonists), including smaller size, increased hydrophobicity and increased hydrogen bond features (Ekins et al., 2008).

The significant side effects of ketoconazole are largely due to its off-target effects (e.g., cortisol synthesis, hepatic toxicity), some of which are related to its effects as a cytochrome P450/steroid enzyme inhibitor (these effects are also dependent on the stereochemistry of the entire molecule; in particular, the imidazole moiety), and others of which are related to the formation of the N-desmethyl-metabolite (Buchi et al., 1986; Rodriguez and Acosta, 1997; Rodriguez and Buckholz, 2003; Rodriguez et al., 1999). For example, in mice, the N-desmethyl-metabolite of ketoconazole is primarily responsible for hepatotoxicity. Furthermore, the downregulation of serum amyloid A (SAA 1/2) and hepcidin are the only changes in gene expression that correlate with hepatotoxicity (Casley et al., 2007).

Therefore, we surmise that non-P450 inhibitors, as well as stereoisomers that are less toxic to hepatocytes and/or those that do not produce toxic N-desmethyl-metabolites, would be the first step in obtaining safer compounds that block PXR activation. Keeping these principles in mind, we developed several analogs of ketoconazole. One analog, compound 3 (FLB-12; Cpd 3) (Das et al., 2008), which lacks the imidazole group, retained PXR antagonist activity while exhibiting markedly reduced CYP3A4 inhibition. Furthermore, we demonstrated that Cpd 3, when compared with ketoconazole, was significantly less toxic to cells *in vitro* (Das et al., 2008). Here, we present data on Cpd 3, which, in contrast to ketoconazole, antagonizes endogenous PXR activation but also has a "limited" antagonist profile on other related orphan and non-

Molecular Pharmacology Fast Forward. Published on April 4, 2011 as DOI: 10.1124/mol.111.071787
This article has not been copyedited and formatted. The final version may differ from this version.

orphan nuclear receptors. Cpd 3 is significantly less toxic to human and murine hepatocytes *in vitro* and *in vivo*. Cpd 3 antagonizes PXR mediated transcription and SN-38 drug resistance *in vitro* and duration of the loss of righting reflex by anesthesia *in vivo*. Furthermore, Cpd 3 attenuates PXR-enhanced acetaminophen hepatotoxicity in mice. Together, these studies demonstrate that it is feasible to design non-toxic PXR antagonists that may be useful not only as probes for PXR biology, but also as potential therapeutics in the treatment of cancer drug resistance and drug toxicity.

Materials and Methods

Materials. LS174T cells were obtained from the American Type Culture Collection (Manassas, VA). Primary hepatocyte cultures for 4- to 6-week-old C57BL/6 mice were isolated using methods previously described with minor modifications of the 2-step perfusion technique (Seglen, 1976). Human hepatocyte(s) were purchased from In Vitro Technologies, Inc. (Baltimore, MD) and maintained in InVitroGrow HI medium. All cell culture, immunochemistry and transfection reagents were purchased from Invitrogen (Carlsbad, CA) unless otherwise indicated. Acetaminophen, pregnenolone-16alpha-carbonitrile (PCN) and fetal bovine serum (FBS) were purchased from Sigma (St. Louis, MO). hPXR-LBD (S247W/S208W/C284W) triple mutant was generated using pM-Gal4-PXR-LBD as previously published (Wang et al., 2008).

Cell survival assay. To measure cell survival, we used the Promega MTS cell proliferation/cytotoxicity assay kit (Madison, WI) and employed a protocol previously published by our laboratory (Mani et al., 2005).

Molecular Pharmacology Fast Forward. Published on April 4, 2011 as DOI: 10.1124/mol.111.071787
This article has not been copyedited and formatted. The final version may differ from this version.

Transactivation assays. These assays were performed in 293T cells as previously published (Huang et al., 2007). In brief, transient transcription assays were carried out in 293T cells co-transfected with plasmids expressing (A) hPXR (B) hPXR triple mutant (S247W/S208W/C284W) (C) mPXR (D) mCAR (E) LXRα (F) FXR (G) ERα and (H) PPARγ with respective reporters, as shown in schematic diagrams (Fig. 1 and 2). After 8 h of transfection, ligands/drugs for respective receptors were added – Cpd 3 (25 μM), and/or rifampicin 10 μM (Rif; hPXR ligand), and/or pregnenolone-16alpha-carbonitrile 10 μM (PCN; mPXR ligand), and/or T0901315 5 μM (LXRα ligand), and/or chenodeoxycholic acid_50 μM (CDCA; FXR ligand), and/or estradiol 20 μM, (E_2; ERα ligand), and/or rosiglitazone 10 μM (Rosi; PPARγ ligand) and/ or TCPOBOP 0.2μM (mCAR ligand) - and incubated for a total period of 48 h. The cells were harvested in passive lysis buffer (Promega, Madison, WI), and luciferase activity was detected using the dual-luciferase reporter assay system from Promega in 20 μl of cell lysate using the Turner Bio-systems 20/20n Luminometer.

UGT Enzymatic Assay. To assess for UGT enzyme activity, the UGT-Glo™ assay (Promega, Madison, WI) was performed using UGT Microsomes™ according to the manufacturer's protocol. The inhibitory activity of UGT1A1 was measured over a concentration range of 0-100 μM of ketoconazole and Cpd 3. Twenty microliter UGT-Glo™ reactions were performed using UGT multi-enzyme substrate (0.4 mM) and microsomes. Two glucuronidation reactions were set up in parallel. Both reactions contained a source of UGT and proluciferin substrate, but only one contained the uridine 5'-diphosphogulcuronic acid (UDPGA). Reactions were incubated at 37ºC for 2 hrs. Luciferin detection reagent plus D-Cystein was added and reading was performed using a plate reader (luminometer). RLU values were background

Molecular Pharmacology Fast Forward. Published on April 4, 2011 as DOI: 10.1124/mol.111.071787
This article has not been copyedited and formatted. The final version may differ from this version.

subtracted and then converted to percent substrate consumed; values were plotted using GraphPad™ Prism. Experiments were repeated three times, each in duplicate.

Time resolved fluorescence resonance energy transfer (TR-FRET) assays. A LanthaScreen time-resolved fluorescence resonance energy transfer (TR-FRET) PXR Competitive Binding Assay was conducted according to the manufacturer's protocol (Invitrogen, Carlsbad, CA). Briefly, at first serial dilutions of test compounds (Cpd3 or KTZ or Rif)(diluted in TR-FRET PXR Assay Buffer; Invitrogen) were dispensed into triplicate wells of a black, non-treated 384 well assay plate (Corning Life Sciences, Lowell, MA). Second, 5 µl of Fluormone PXR Green was added into each well. Finally, 5 µl of a master mix containing hPXR ligand-binding domain, terbium-labeled anti-glutathione-*S*-transferase (final concentration of 10 nM), and dithiothreitol (final concentration of 0.05 mM) was added into each well. The content was mixed briefly (10 s) and the plate was incubated in the dark at room temperature (22-24°C) for one hour. TR-FRET was measured using a SpectraMax® M5 Microplate Reader (Molecular Devices), with the excitation wavelength of 340 nm, emission wavelengths of 520 nm and 495 nm. TR-FRET ratio was calculated by dividing the emission signal at 520 nm by the emission signal at 495 nm. Data are expressed as a TR-FRET ratio. Error bars represent the SEM of duplicate wells from two separate experiments. The curve was fit to data (TR-FRET ratio *vs* log test compound) using a sigmoidal dose response (variable slope) equation in GraphPad™ Prism software.

Co-activator-dependent receptor ligand assays. hPXR LBD ^{35}S methionine-labeled proteins were prepared using in vitro transcribed and translated protein (TNT, Promega). The GST-SRC-1 protein was expressed in *E. coli* BL21 cells and purified using glutathione-sepharose (Amersham Biosciences, Piscataway, NJ) and pull down experiments performed as

Molecular Pharmacology Fast Forward. Published on April 4, 2011 as DOI: 10.1124/mol.111.071787
This article has not been copyedited and formatted. The final version may differ from this version.

described previously (Huang et al., 2007). In brief, Purified GST fusion protein (5 µg) was incubated with 5 µl of in vitro translated ^{35}S-labeled protein with overnight shaking at 4 °C in the presence of 0.2% DMSO (vehicle), rifampicin (10 µM) or Cpd3 (25 µM) or combination of rifampicin and Cpd3. GST beads were used as a negative control. The bound protein was washed three times and the beads were collected by centrifugation at 3,000 rpm for 5 minutes. The bound protein was eluted into SDS sample buffer, and then subjected to 10% SDS-PAGE, and the gel was processed has reported previously (Huang et al., 2007). Each experiment was repeated twice and each blot was exposed for a minimum of three times.

RNA preparation and RT-Quantitative PCR assays. LS174T cells were treated with rifampicin (10 µM) or rifampicin (10 µM) plus Cpd 3 (20 µM) or DMSO and after 48 h total RNA was extracted from cells with Qiagen RNeasy Mini kit (Qiagen Inc., Valencia, CA), according to the manufacturer's instructions. Wild-type C57BL/6 mice were treated with DMSO or ketoconazole or Cpd 3 for (300 mg/kg/day) for 3 days and then the animals were scarified and total RNA was isolated from the liver using the QIAzole, Qiagen RNeasy Mini kit, according the Qiagen protocol. Two micrograms of total RNA was reverse transcribed with random hexamer primers and SuperScript^{TM} III-RT (Invitrogen, Carlsbad, CA). The RT-quantitative PCR for MDR1, CYP3A4, UGT1A1, hepcidins, SAA (Serum amyloid A) and β-actin was performed using TaqMan universal PCR master mix and TaqMan probes, as previously described (Gupta et al., 2008; Huang et al., 2007). The following assays are available on demand were procured from applied bio-system, CYP3A4 Hs00604506_ml, MDR1 Hs00184500_ml, UGT1A1 Hs02511055_s1, ACTB 4333762, Hepcidin-1 Mm00519025_ml, Hepcidin-2 Mm00842044_gl, SAA1 Mm00656927_gl, SAA3 Mm00441203_ml, GAPDH Mm999999915_g1. PCR reaction conditions for assays were 50°C for 2 min, 95°C for 10 min, followed by 40 cycles of

Molecular Pharmacology Fast Forward. Published on April 4, 2011 as DOI: 10.1124/mol.111.071787
This article has not been copyedited and formatted. The final version may differ from this version.

amplification (95°C for 15 s, then 60°C for 1 min). The relative fold change in mRNA expression in treated samples compared with controls was calculated using comparative Ct method. The percent inhibition (antagonism) was calculated using the difference in fold expression in rifampicin- *vs* rifampicin + Cpd 3-treated cells, subsequently divided by fold expression in rifampicin-treated cells (x 100 %).

Animal studies. C57BL/6 mice (6-8 weeks old) (Jackson Labs, Bar Harbor, Maine) were used for all animal studies. The transgenic and knockout mice have been described before and the loss of righting reflex studies were performed as previously published (Huang et al., 2007) (The transgenic and knockout mice were obtained from Dr.Wen Xie , University of Pittsburgh, PA). Oral (gavage) dosing of Cpd 3 (100, 200, 300, 600 mg/kg) and ketoconazole (100, 200, 300, 600 mg/kg) was performed using drugs solubilized in corn oil and dosed twice per day for 4 days. Mice were euthanized on day 4 and serum and liver were isolated for the estimation of liver enzyme activity, H&E staining and gene expression studies (qRT-PCR and immunoblot). For the serum transaminase studies and gene expression studies in the mouse liver, fixed doses of 300 mg/kg of ketoconazole and Cpd 3 were used, respectively. LORR studies were performed as previously described (Huang et al., 2007). For LORR studies, the Cpd 3 dose was 300 mg/kg/day. For studies pertaining to acetaminophen (APAP) toxicity, the dose and schedule of administration of acetaminophen was directly adopted from a prior published study (Guo et al., 2004). In these studies, Cpd 3 (300 mg/kg/day administered in two divided doses/day) was started on day –1 prior to PCN dosing (75 mg/kg, ip for two days) and continued through acetaminophen dosing (350 mg/kg, ip) for a total of 4 days. For $pxr^{+/+}$, seven treatment groups (8mice/group) were developed: vehicle control (100% corn oil), PCN, Cpd 3, APAP, PCN + APAP, Cpd 3 + APAP, and PCN + Cpd 3 + APAP. Total blood and serum were isolated at 24

Molecular Pharmacology Fast Forward. Published on April 4, 2011 as DOI: 10.1124/mol.111.071787
This article has not been copyedited and formatted. The final version may differ from this version.

hours post-acetaminophen dosing for the assessment of ALT levels.

Immunoblot. Individual or pooled livers from the treated groups of Cpd3 and KTZ has mentioned in animal studies method (six mice in each group) were homogenized on ice in Tris-HCl buffer (0.01 M, pH 7.4) containing protease inhibitors cocktail (P8340, Sigma Aldrich). The homogenate was centrifuged at 4,000g for 10 min (4°C), the pellet was discarded, and the supernatant was centrifuged at 100,000g for 30 min (4°C). The resulting pellet was re-suspended in Tris-HCl buffer with protease inhibitors cocktail, expression of MDR1 (anti-P-gp -C219, Signet Labs, Dedham, MA) and Na^+/K^+- ATPase (loading control) (sc-28800, Santa Cruz Biotechnology, Santa Cruz, CA) were performed as previously reported by Huang et al., 2007.

LC/MS/MS. Blood and tissue samples were analyzed using ESCi multi-mode ionization (Waters TQ Tandem Quadrupole Mass Spec, Waters Corp, Parsippany, NJ). The best ionization was achieved by positive ion electrospray. The MS/MS detection was developed and optimized using IntelliStart™ Software. Anthracene-2 was used as internal standard (Supplemental Fig. 8). The elution peak for compound 3 occurred at 1.15 minutes and also contained an isomer peak (at 1.13 minutes). To demonstrate sensitivity, a linear calibration curve was created by serial dilutions of the stock standard (1-1000 ng/ml) in mouse blood plasma (data not shown; r^2 = 99.9091 x 10^{-2}). The lower limit of quantitation (LLQ) for this assay is 5 pg on the column, with a signal/noise (S/N) ratio of 168.00. Tissue concentrations were established by normalizing to total protein content (NanoDrop 1000 Spectrophotometer, Thermo Scientific, and Waltham, MA) in cleared lysate (membrane-free) injected into columns.

Transaminase enzymatic assay. Mouse serum was collected and prepared according to the manufacturer's instructions for the MaxDiscovery™ Alanine (ALT) and Aspartate (AST)

Molecular Pharmacology Fast Forward. Published on April 4, 2011 as DOI: 10.1124/mol.111.071787
This article has not been copyedited and formatted. The final version may differ from this version.

Transaminase enzymatic assay kit (Bio-Scientific Corp, Austin, TX). A standard curve was also generated using the pyruvate control dilutions, and enzymatic activity in serum samples was reported in units per liter. Measurements were performed on a SpectraMax® M5 Microplate Reader (Molecular Devices).

Manual Patch Clamp assay. Whole cell patch-clamp recordings were made at 37± 2ºC from human embryonic kidney (HEK) 293 cells stably transfected with hERG gene, maintained in culture with selective agent (G148, Sigma-Aldrich, St-Louis). The cells were transferred to a bath mounted onto the heated stage of an inverted microscope. The bath was perfused with an external solution comprised of (mM) NaCl 140, KCl 5, $CaCl_2$ 1.8, $MgCl_2$ 1, Glucose 10 and HEPES 10 (pH 7.4). The electrodes used were pulled from borosilicate glass using a micropipette puller (PMP-202, MicroData Instruments Inc. S. Plainfield, New Jersey) and filled with internal pipette solution containing (in mM) KCl 140, $MgCl_2$ 1, EGTA 5, HEPES 10, Mg-ATP 4 and sucrose 10. The resistance of the electrode was 5-8 MΩ prior to touching the cell membrane. Currents were acquired at a rate of 2 Hz, and filtered using a low-pass 4-pole Bessel filter with cut-off rate set at 650 Hz. Baseline condition currents were recorded using the PClamp 10 acquisition suite (Molecular Devices, Sunnyvale, CA) after achieving a GΩ seal, following a 2-minute equilibration period. Currents were also recorded after 5 minutes of exposure to each concentration of ketoconazole (Sigma-Aldrich, St-Louis) or Cpd3. The cells were stimulated every 10 seconds with the pulse as denoted in Fig. 1A. Current analysis was performed on digitized current records using Clampfit 10. Current peak, activation, inactivation and deactivation constants were calculated automatically by the software. Repeat student's t-tests

Molecular Pharmacology Fast Forward. Published on April 4, 2011 as DOI: 10.1124/mol.111.071787
This article has not been copyedited and formatted. The final version may differ from this version.

were used to assess statistical significance in changes from baseline conditions. Statistical significance was declared when $P \leq 0.05$.

Electrochemiluminescence. MSD's chemiluminescence detection technology (www.mesoscale.com; Gaithersburg, MD) was employed to measure ERK (total, sc-93, C-16), phospho ERK (sc-7383, E-4), in lysate of LS174T cells after cell exposed to Cpd3 or KTZ (0-25μm) or vehicle control. Cell lysate (5 μg) was coated on 96-well MULTI-ARRAY MSD high bind plates according to manufacturer's instructions. The wells were incubated at room temperature for 2 hour, and then blocked with MSD Blocker 'A' solution diluted in PBS for 1 hour at room temperature. After incubation with primary antibody (1 μg/ml) for 1hour at room temperature, the wells were washed with Blocker 'A' solution and then incubated with the secondary antibody (1 μg/ml). After an additional 1h of incubation, the wells were washed and refilled with 150 μl MSD Read Buffer (1x) with surfactant. Readings were measured using the SECTOR Imager 2400 according to manufacturer's instructions and signals (light units) were plotted against the different concentration of compounds to phospho ERK expression. Experiments were performed in duplicate and repeated twice. Anti-ERK1/2 and FRS2 antibody were used to normalize the data for protein loading.

Statistical analysis. Student's t Test (two tailed;α, β =0.05) was used to analyze differences between two groups. Trends analyses between three or more groups were performed using ANOVA test. All the results were expressed as means ± SEM. *P* value of less than 0.05 was considered to be significant. All analyses were performed using GraphPad Prism software.

Molecular Pharmacology Fast Forward. Published on April 4, 2011 as DOI: 10.1124/mol.111.071787
This article has not been copyedited and formatted. The final version may differ from this version.

Results

Cpd 3 antagonizes PXR activation *in vitro*. Cpd 3 has been shown to antagonize PXR activation in transformed hepatocyte cell lines (Das et al., 2008). Furthermore, this compound is significantly less toxic to cells than ketoconazole (KTZ) (Das et al., 2008). However, its effect on endogenous PXR activation is unknown. First, using the TR-FRET assay, we demonstrate that the Cpd3 does not quench fluorescence, suggesting low affinities for binding and competing with strong ligands within the ligand binding pocket (Fig. 1A). However, Cpd 3 (25 μM) was found to significantly antagonize rifampicin (10 μM) mediated activation of human PXR in a PXR-transactivation assay (Fig. 1B). Since full-length PXR cannot be purified from mammalian systems, we employed a genetic approach towards determining whether Cpd3 may bind outside the ligand binding pocket, as suggested by experiments in Fig 1 A & B. We used a PXR ligand-binding pocket triple mutant plasmid (S247W/S208W/C284W) which was constructed by mutating three amino acids to more bulky amino acid (tryptophan) at positions S247/S208/C284, resulting in ligand binding occlusion, and by serendipity, ligand-independent constitutive activation (Chrencik et al., 2005; Wang et al., 2008). We found that Cpd3 (25 μM) significantly antagonized hPXR-LBD triple mutant in the PXR-transactivation assay (Fig. 1C), which implies that PXR is likely antagonized by Cpd3 at a site distinct from the ligand-binding pocket. Indeed, Cpd3 is able to disrupt the interaction between PXR and SRC-1 on a protein pulldown assay (Supplemental Fig. 1A).

To determine whether endogenous PXR is antagonized by Cpd 3, LS174T cells were exposed to rifampicin (10 μM) and/or ketoconazole (25 μM) or Cpd 3 (25 μM). After 48 h of exposure to drug(s), total RNA was isolated from treated cells and subjected to RT-qPCR of the

Molecular Pharmacology Fast Forward. Published on April 4, 2011 as DOI: 10.1124/mol.111.071787
This article has not been copyedited and formatted. The final version may differ from this version.

PXR target genes CYP3A4, MDR1 and UGT1A1. The human PXR ligand, rifampicin, induces a 16.3, 18.2 and 6.3 fold mean change in CYP3A4, MDR1 and UGT1A1 mRNA abundance, respectively (Fig. 1D). Cpd 3 alone induces the expression of MDR1 (3.8-fold), but has negligible effect on CYP3A4 (1.8-fold) and UGT1A1 (1.7-fold). Importantly, there is no apparent induction of MDR1 protein by Cpd3 in mouse liver, suggesting lack of significant induction of MDR1 in vivo (Supplemental Fig. 1B). However, in the presence of rifampicin, Cpd 3 inhibits rifampicin-mediated CYP3A4, MDR1 and UGT1A1 transcription by ~76%, 79%, and 60%, respectively.

Cpd 3 effects on orphan receptor mediated transcription *in vitro*. We have shown previously that ketoconazole antagonizes the ligand-mediated activation of mPXR, CAR, LXR, and FXR (receptors closely related to PXR); however, there was no effect on ERα or PPARγ mediated activation (Huang et al., 2007). Cpd 3 (25 μM) was found to inhibit the PCN (10 μM) mediated activation of mPXR (Fig. 2A), whereas it did not show any significant inhibitory effects on the ligand-mediated activation of LXR (T0901315 5 μM) (Fig. 2B), FXR (chenodeoxycholic acid_50 μM) (Fig. 2C), ERα (estradiol 20 μM) (Fig. 2D), PPARγ (rosiglitazone 10 μM) (Fig. 2E) and mCAR (TCPOBOP 0.2μM) (Fig. 2F) in our reporter assays. Notably, Cpd 3 did not significantly activate these nuclear receptors (Fig. 2B-F).

LC/MS/MS of Cpd 3 in the liver, blood and intestine. The LC and MS-MS spectrum for Cpd 3 is shown in Supplemental Fig. 2. Compound 3 is orally absorbed in mice. A single oral dose of compound 3 (200 mg/kg) yields an $AUC_{(0\text{-}t)}$ ~ 121.7 (blood), 254.9 (liver), and 537.7 (proximal small bowel) $\mu M.h^{-1}$ (Supplemental Fig. 3). This suggests that there is either accumulation and/or persistence of drug in these tissue compartments. At 2 hours (h) post-

Molecular Pharmacology Fast Forward. Published on April 4, 2011 as DOI: 10.1124/mol.111.071787
This article has not been copyedited and formatted. The final version may differ from this version.

dosing, the drug concentration in blood and tissues ranges from ~25.4 to 38.1 μM, respectively. At 48 h, there is virtually no drug in the blood compartment (< LLQ); however, the concentrations in the tissues range from 0.5 to 1.9 μM. The approximate half-life of Cpd 3 is ~ 0.53 (blood), 0.77 (liver), and 8.59 (proximal small bowel) h. This implies that oral dosing (multiple times per day e.g., twice per day or BID) would be necessary to maintain tissue levels in the micromolar range (one exponential phase, r^2 ~ 0.99; GraphPad Prism software; Supplemental Fig. 3). These data also suggest that there are tissue-specific residence times for the drug and perhaps highly metabolic tissues like blood and liver clear the drug faster than other tissues. Therefore, we made the assumption that if we increased the dose of Cpd 3 and administered the compound at least three times per day, after 2 or more days of continuous dosing, steady-state trough levels should approximate ~ >10 μM. Accordingly, we chose to perform a second experiment, in which we dosed mice at 300 mg/kg three times per day by gavage. However, after one day we reduced the frequency to two times per day due to significant throat irritation in > 90% of mice. The total number of doses delivered prior to sacrificing the mice was 8. The mice were sacrificed 10 h after the last delivered dose by gavage. Since steady states for most drugs are usually reached after approx ~ $5.t_{1/2}$, we surmised that, at this point, all mice would exhibit steady-state blood and tissue concentrations of Cpd 3. The blood and tissue concentrations after 8 doses of Cpd 3 are shown in Table 1.

Cpd 3, unlike ketoconazole, is significantly less toxic to hepatocytes *in vitro* and *in vivo*. At concentrations > 10 μM, Cpd 3 is significantly less toxic to primary mouse (Fig. 3A) and human (Fig. 3B) hepatocytes. Indeed, vacuolization and cellular ballooning is a hallmark of drug-induced toxicity (Lee, 1995) and ketoconazole hepatotoxicity (Lewis et al., 1984). On H & E stained sections of mice livers exposed to multiple doses of Cpd 3 or ketoconazole, it is

Molecular Pharmacology Fast Forward. Published on April 4, 2011 as DOI: 10.1124/mol.111.071787
This article has not been copyedited and formatted. The final version may differ from this version.

evident that there is a profound increase in vacuolization and cellular ballooning at ketoconazole doses $\geq$ 200 mg/kg [~ $\geq$ 10 μM]; however, these effects are only beginning to be seen at concentrations of Cpd 3 ~ $\geq$ 23 μM. At the highest dose delivered, 600 mg/kg of both ketoconazole and Cpd 3, there was significant cellular ballooning in the ketoconazole exposed mice. There was a less dramatic effect on livers exposed to Cpd 3 (Fig. 3C). At this dose, the mouse livers and sera were isolated and tissue was extracted for gene expression and enzymatic assays, respectively. Cpd 3, unlike ketoconazole, does not inhibit expression of hepcidin-1 & 2 and SAA-1 & 3 (Fig. 3D). In addition, high serum levels of ALT and AST were statistically significant only in the ketoconazole-treated mice. The Cpd 3 exposed mice had AST (Fig. 3E) and ALT (Fig. 3F) levels similar to those of control treated mice.

Cpd 3 inhibits PXR mediated SN-38 drug resistance in colon cancer cells *in vitro*. Previously published data have demonstrated that PXR ligands, such as rifampicin, can induce increased resistance to SN-38 mediated cytotoxicity, in part through enhanced glucuronidation via UGT1A1 (Gupta et al., 2008; Raynal et al., 2010). We exposed the colon cancer cells LS174T (high endogenous PXR) (transduced with Scrambled shRNA or PXR shRNA, Supplemental Fig. 4 & 5) to vehicle, SN-38, and/or rifampicin (10) and/or Cpd 3 (25) (Fig. 4A & B). The data show that Cpd 3 significantly inhibits rifampicin-mediated effects on the cytotoxicity of SN-38 in scrambled shRNA cells (SN-38/Rif *vs* SN-38/Rif/Cpd 3, One-way ANOVA, P <0.00001) (Fig. 4A). Cpd 3 did not alter rifampicin induced SN-38 cytotoxicity in PXR shRNA cells (Fig. 4B). In this context, since azole compounds inhibit CYP450 and UGT enzymes, which could independently affect SN-38 pharmacodynamics in cells, it has been previously noted that ketoconazole inhibits UGT1A1 and UGT1A9 (Yong et al., 2005); however, Cpd 3 has no

Molecular Pharmacology Fast Forward. Published on April 4, 2011 as DOI: 10.1124/mol.111.071787
This article has not been copyedited and formatted. The final version may differ from this version.

significant effects on UGT1A1 activity (a major determinant of SN-38 detoxicification in cells) (Supplemental Fig. 6).

Cpd 3 antagonizes PXR activation *in vivo*. Previously published data have established that ketoconazole reverses the duration of the loss of righting reflex mediated by PXR ligands in *pxr* $^{(+/+)}$ and *humanized (h) PXR* mice, but not in *pxr* $^{(-/-)}$ mice (Huang et al., 2007). In this assay, the consequences of activating PXR can be studied using mice challenged with 2,2,2-tribromoethanol (Avertin) anesthesia, where the drug-induced change in the duration of the loss of righting reflex (LORR) acts as a phenotypic measure of PXR target gene activity and xenobiotic metabolism (Huang et al., 2007). We verified that the effects of ketoconazole were pxr-specific by comparing wild-type (*pxr* $^{(+/+)}$) and *pxr*-null (*pxr* $^{(-/-)}$) mice. We used the same assay to study the effects of Cpd 3 on this pxr mediated phenotype *in vivo*. Since Cpd 3 inhibits both human and mouse pxr (when ligand tethered), we performed LORR studies in all three genotypes: *pxr* $^{(+/+)}$, *humanized (h) PXR* and *pxr* $^{(-/-)}$. The data indicate that Cpd 3 reverses the duration of LORR mediated by a pxr/PXR ligand only in the *pxr* $^{(+/+)}$ (Fig. 4C) *hPXR* (Fig. 4D), but not in *pxr* $^{(-/-)}$ (Fig. 4D). These results indicate that (a) Cpd 3 antagonizes pxr/PXR function *in vivo* and (b) Cpd 3 has pxr/PXR specific effects *in vivo*.

A second model to study the in vivo activation effects of PXR in the liver has been demonstrated by prior work that shows a significant enhancement of acetaminophen-induced liver toxicity in mice (Guo et al., 2004) (Cheng et al., 2009; Wolf et al., 2005). In this model, *pxr*$^{+/+}$ were pretreated with the pxr activator PCN for two days before administration of one APAP intraperitoneal (i.p.) dose dissolved in alkaline solution. Cpd 3 was administered one day before administration of PCN and continued for a total of 4 days. The mice were sacrificed at 24

Molecular Pharmacology Fast Forward. Published on April 4, 2011 as DOI: 10.1124/mol.111.071787
This article has not been copyedited and formatted. The final version may differ from this version.

hours post APAP administration and blood was immediately aspirated from a cardiac puncture for determination of ALT levels (see Materials and Methods). In *pxr*$^{+/+}$ mice, PCN significantly augments APAP-induced ALT levels, signifying hepatotoxicity (Fig. 5; **P* < 0.05). These data also indicate that Cpd 3 abrogates PCN-mediated APAP hepatotoxicity (Fig. 5; ***P* <0.05).

Effect of Cpd3 and Ketoconazole on hERG current amplitude. hERG currents activate in an upward curve following depolarization, and deactivate/inactivate when the cells' holding potential is brought back to -90 mV (Fig. 6A). Ketoconazole and Cpd 3 caused concentration-dependent decreases in hERG activating current density. A shift in voltage for the activation curve was observed for both compounds, which suggests that both ketoconazole and Cpd 3 were more potent hERG inhibitors at more depolarized holding potentials. In addition, Ketoconazole and Cpd3 produced a concentration-dependent inhibition of hERG tail current density. At the peak of the I/V curve (measured immediately following the reporlarization of the cells), Ketoconazole inhibited 69% of the current, while Cpd3 inhibited 42% of the hERG current at the peak of the I/V curve, at approximately +7 mV. The IC50 for ketoconazole was 18 µM but IC50 for Cpd3 not available (Fig 6B) and (Table 2 and 3). The reversal potential for the current was extrapolated to -98 mV, close to the theoretical reversal potential calculated to be -85 mV. It did not vary following exposure to either ketoconazole or Cpd3, suggesting that neither molecule alters the selectivity of the channels.

Effect of Cpd3 and Ketoconazole on hERG activation, deactivation, and inactivation kinetics. Ketoconazole caused a concentration-dependent deceleration in hERG activation, an effect which was not observed with Cpd3. This translated into a hERG current which activated more slowly and reached a lower level in the presence of ketoconazole. In contrast, the activating

Molecular Pharmacology Fast Forward. Published on April 4, 2011 as DOI: 10.1124/mol.111.071787
This article has not been copyedited and formatted. The final version may differ from this version.

current measured in the presence of Cpd3 was lower, but activated at the same rate regardless of the concentration of Cpd3 present in the bath (Fig. 7).

Neither Ketoconazole nor Cpd3 had any effect on the deactivation and inactivation kinetics of the current. Inactivation kinetics decelerated with voltage, but varying concentrations of either ketoconazole or Cpd3 did not enhance the inactivation kinetics of the currents. It is a coincidence that the currents which inactivate faster were used to test Cpd3, leading to inactivation constant values (TAU) which were lower for Cpd3 currents (i.e. faster inactivation). Regardless of the rate of inactivation, statistical tests confirmed that the current kinetics exhibited identical pharmacological sensitivity to Ketoconazole and Cpd3 (data not shown).

Discussion

Inappropriate PXR activation has some undesired and important pathophysiologic consequences (e.g., promoting drug interactions that alter drug pharmacokinetics, efficacy and toxicity, and cancer drug resistance). In addition, there is a lack of non-toxic PXR antagonists that would allow researchers to chemically reduce the activity of PXR in different biologic systems, so that its molecular consequences may be fully characterized. Hence, from a biological and clinical perspective, developing PXR specific antagonists is an important but daunting task. Based on some well-known observations about the chemical moieties of ketoconazole, we explored the possibility of first developing less toxic analogs of ketoconazole that still served as PXR antagonists. We demonstrated that imidazole moiety deleted analogs of ketoconazole are less toxic to cells. Further modifications of the halogen on the phenyl group led to the discovery of compounds that could inhibit PXR but not CYP3A4 (Das et al., 2008).

Molecular Pharmacology Fast Forward. Published on April 4, 2011 as DOI: 10.1124/mol.111.071787
This article has not been copyedited and formatted. The final version may differ from this version.

One lead compound, Cpd 3, was demonstrated to abrogate endogenous PXR activation *in vitro* and *in vivo* and was less toxic to liver cells *in vivo* when compared with ketoconazole. Indeed, markers of azole-mediated hepatotoxicity (e.g., liver enzymes, Hepcidin and SAA expression profile) suggested that Cpd3 was likely to have significantly less toxic effect on the liver than ketoconazole. Importantly, Cpd 3 did not inhibit mCAR, LXR and FXR to the same extent to ketoconazole (Huang et al., 2007), which suggests that there are analogs that could be made more PXR specific without compromising their inhibitory potency.

Ketoconazole has off-target effects on many enzymes and protein channels (e.g., CYP450, UGTs, 11β-hydroxylases, BK channels, hERG) (Loose et al., 1983; Nardi and Olesen, 2008; Power et al., 2006; Yong et al., 2005; Yoshida and Niwa, 2006). To begin to explore some of the off-target properties of Cpd 3, as compared to ketoconazole, we evaluated the potency of ketoconazole and Cpd 3 in modifying hERG current density and current kinetics. The data presented herein suggest that Cpd3 is significantly less potent than ketoconazole at inhibiting the hERG tail current. Both ketoconazole and Cpd3 exhibit voltage-dependent hERG tail current inhibition, with a more pronounced effect at more depolarized potentials. This effect may translate into a decreased repolarization reserve, since the demand for hERG current in vivo is greatest at the end of Phase 0 of the action potential, when the cardiac cells are maximally depolarized. Unfortunately, this is also a window of membrane potentials where the cardiac cells in the ventricles spend a significant amount of time (approximately 350 ms per heartbeat). The loss of repolarization from ketoconazole exposure is expected to be greater than from Cpd3; ketoconazole is twice as potent as Cpd3 at decreasing current peak, and the activation of the current is decreased for ketoconazole treated samples (but not Cpd3). This is likely to lead to a greater decrease in charge transport (the area under the activating current curve) for

Molecular Pharmacology Fast Forward. Published on April 4, 2011 as DOI: 10.1124/mol.111.071787
This article has not been copyedited and formatted. The final version may differ from this version.

ketoconazole. The kinetics of deactivation/inactivation was not affected by the compounds tested.

Another important effect of ketoconazole is its inhibition of CYPs (e.g., CYP3A4), and UGTs (e.g., UGT1A1). We have extended our findings to show that Cpd 3 does not significantly inhibit UGT1A1 (Supplemental Fig. 6). Hence, it is possible to change the activity of analogs to several non-receptor protein targets without affecting their potency toward the target protein of interest, PXR. Indeed, Cpd 3 increased the cytotoxicity of SN-38/Rif in colon cancer due to its effects on PXR rather than azole-mediated (e.g., ketoconazole-mediated) inhibition of CYP3A4 (Das et al., 2008) and/or UGT1A1 (Fig S6) (Yong et al., 2005).

On the other hand, some properties relating to ketoconazole's chemical structure have potential pharmacological benefits in human pathophysiology (e.g., BK channels are pharmacological targets for stroke treatment). For example, some structural variants of ketoconazole block or potentiate BK channel (Maxi-K or slo-1) activity. This property is dependent on phenyl and phenoxy moieties and the imidazole moiety is not important (Nardi and Olesen, 2008; Power et al., 2006). Hence, Cpd 3, which lacks the imidazole moiety but has preserved its phenyl group, may still have an effect on these channels. In addition, there are several other enzyme/protein systems/networks that are affected by ketoconazole (Gergely et al., 1984; Kinobe et al., 2006; Loose et al., 1983; Rodriguez and Buckholz, 2003; Rodriguez et al., 1999; Yoshida and Niwa, 2006), but current evidence suggests that the loss of the imidazole moiety might not adversely affect the pharmacological properties of Cpd 3 in human applications. However, further studies are needed to profile the effects of ketoconazole and Cpd 3 on all human NRs and special channel proteins like BK, and Kv1.5. In this context, it is

Molecular Pharmacology Fast Forward. Published on April 4, 2011 as DOI: 10.1124/mol.111.071787
This article has not been copyedited and formatted. The final version may differ from this version.

important to note that Cpd3, unlike ketoconazole, has negligible (inductive) effect on phosphorylation of ERK, a common downstream effector of GPCRs and other relevant receptor targeted pathways (Supplemental Fig 7) (Chong et al., 2004; Leroy et al., 2007; Osmond et al., 2005). Finally, it would be important to study the metabolism of radiolabeled compound 3 to determine the production of desmethyl metabolites *in vitro* and *in vivo.*

In summary, our findings validate the feasibility of developing non-toxic inhibitors of the adopted orphan nuclear receptor PXR. It is also feasible to design analogs that have fewer off-target effects on cross-talking nuclear receptors. These drugs will not only serve as valuable chemical tools for probing PXR action *in vitro* and *in vivo,* but also be important adjuncts for novel targeted approaches against cancer drug resistance and other drug-related toxicities (e.g., acetaminophen hepatotoxicity). Since environmental xenogens (e.g, Bisphenol A) are commonly found in humans at concentrations that could potentially activate PXR, the notion that some of the PXR-mediated pathophysiological processes could have clinical utility now seems justified (Cobellis et al., 2009; Creusot et al.; Takeshita et al., 2001).

Acknowledgments

We thank Dr. Ronald Evans, Dr. Wen Xie (for pxr knockout and humanized PXR mice), and Dr. Prem Reddy for reagents.

Authorship Contributions

Participated in research design: Venkatesh, Cayer , Salvail and Mani
Conducted experiments: Venkatesh, Wang, Cayer, Leroux
Contributed new reagents or analytic tools: Das
Performed data analysis: Venkatesh, Cayer ,Salvail and Mani
Wrote or contributed to the writing of the manuscript: Venkatesh, Cayer , Salvail and Mani
Other: Mani acquired funding for the research.

Molecular Pharmacology Fast Forward. Published on April 4, 2011 as DOI: 10.1124/mol.111.071787
This article has not been copyedited and formatted. The final version may differ from this version.

References

Biswas A, Mani S, Redinbo MR, Krasowski MD, Li H and Ekins S (2009) Elucidating the 'Jekyll and Hyde' nature of PXR: the case for discovering antagonists or allosteric antagonists. *Pharm Res* **26**(8):1807-1815.

Buchi KN, Gray PD and Tolman KG (1986) Ketoconazole hepatotoxicity: an in vitro model. *Biochem Pharmacol* **35**(16):2845-2847.

Casley WL, Ogrodowczyk C, Larocque L, Jaentschke B, LeBlanc-Westwood C, Menzies JA, Whitehouse L, Hefford MA, Aubin RA, Thorn CF, Whitehead AS and Li X (2007) Cytotoxic doses of ketoconazole affect expression of a subset of hepatic genes. *J Toxicol Environ Health A* **70**(22):1946-1955.

Cheng J, Ma X, Krausz KW, Idle JR and Gonzalez FJ (2009) Rifampicin-activated human pregnane X receptor and CYP3A4 induction enhance acetaminophen-induced toxicity. *Drug Metab Dispos* **37**(8):1611-1621.

Chong MP, Barritt GJ and Crouch MF (2004) Insulin potentiates EGFR activation and signaling in fibroblasts. *Biochem Biophys Res Commun* **322**(2):535-541.

Chrencik JE, Orans J, Moore LB, Xue Y, Peng L, Collins JL, Wisely GB, Lambert MH, Kliewer SA and Redinbo MR (2005) Structural disorder in the complex of human pregnane X receptor and the macrolide antibiotic rifampicin. *Mol Endocrinol* **19**(5):1125-1134.

Cobellis L, Colacurci N, Trabucco E, Carpentiero C and Grumetto L (2009) Measurement of bisphenol A and bisphenol B levels in human blood sera from healthy and endometriotic women. *Biomed Chromatogr* **23**(11):1186-1190.

Creusot N, Kinani S, Balaguer P, Tapie N, LeMenach K, Maillot-Marechal E, Porcher JM, Budzinski H and Ait-Aissa S (2010) Evaluation of an hPXR reporter gene assay for the

detection of aquatic emerging pollutants: screening of chemicals and application to water samples. *Anal Bioanal Chem* **396**(2):569-583.

Das BC, Madhukumar AV, Anguiano J, Kim S, Sinz M, Zvyaga TA, Power EC, Ganellin CR and Mani S (2008) Synthesis of novel ketoconazole derivatives as inhibitors of the human Pregnane X Receptor (PXR; NR1I2; also termed SXR, PAR). *Bioorg Med Chem Lett* **18**(14):3974-3977.

Ekins S, Chang C, Mani S, Krasowski MD, Reschly EJ, Iyer M, Kholodovych V, Ai N, Welsh WJ, Sinz M, Swaan PW, Patel R and Bachmann K (2007) Human pregnane X receptor antagonists and agonists define molecular requirements for different binding sites. *Mol Pharmacol* **72**(3):592-603.

Ekins S, Kholodovych V, Ai N, Sinz M, Gal J, Gera L, Welsh WJ, Bachmann K and Mani S (2008) Computational discovery of novel low micromolar human pregnane X receptor antagonists. *Mol Pharmacol* **74**(3):662-672.

Gergely P, Nekam K, Lang I, Kalmar L, Gonzalez-Cabello R and Perl A (1984) Ketoconazole in vitro inhibits mitogen-induced blastogenesis, antibody-dependent cellular cytotoxicity, natural killer activity and random migration of human leukocytes. *Immunopharmacology* **7**(3-4):167-170.

Guo GL, Moffit JS, Nicol CJ, Ward JM, Aleksunes LA, Slitt AL, Kliewer SA, Manautou JE and Gonzalez FJ (2004) Enhanced acetaminophen toxicity by activation of the pregnane X receptor. *Toxicol Sci* **82**(2):374-380.

Gupta D, Venkatesh M, Wang H, Kim S, Sinz M, Goldberg GL, Whitney K, Longley C and Mani S (2008) Expanding the roles for pregnane X receptor in cancer: proliferation and drug resistance in ovarian cancer. *Clin Cancer Res* **14**(17):5332-5340.

Harmsen S, Meijerman I, Febus CL, Maas-Bakker RF, Beijnen JH and Schellens JH (2009) PXR-mediated induction of P-glycoprotein by anticancer drugs in a human colon adenocarcinoma-derived cell line. *Cancer Chemother Pharmacol* **66**(4):765-771.

Huang H, Wang H, Sinz M, Zoeckler M, Staudinger J, Redinbo MR, Teotico DG, Locker J, Kalpana GV and Mani S (2007) Inhibition of drug metabolism by blocking the activation of nuclear receptors by ketoconazole. *Oncogene* **26**(2):258-268.

Kinobe RT, Dercho RA, Vlahakis JZ, Brien JF, Szarek WA and Nakatsu K (2006) Inhibition of the enzymatic activity of heme oxygenases by azole-based antifungal drugs. *J Pharmacol Exp Ther* **319**(1):277-284.

Kortagere S, Krasowski MD, Reschly EJ, Venkatesh M, Mani S and Ekins (2010) S Evaluation of computational docking to identify pregnane X receptor agonists in the ToxCast database. *Environ Health Perspect* **118**(10):1412-1417.

Lee WM (1995) Drug-induced hepatotoxicity. *N Engl J Med* **333**(17):1118-1127.

Leroy D, Missotten M, Waltzinger C, Martin T and Scheer A (2007) G protein-coupled receptor-mediated ERK1/2 phosphorylation: towards a generic sensor of GPCR activation. *J Recept Signal Transduct Res* **27**(1):83-97.

Lewis JH, Zimmerman HJ, Benson GD and Ishak KG (1984) Hepatic injury associated with ketoconazole therapy. Analysis of 33 cases. *Gastroenterology* **86**(3):503-513.

Loose DS, Stover EP and Feldman D (1983) Ketoconazole binds to glucocorticoid receptors and exhibits glucocorticoid antagonist activity in cultured cells. *J Clin Invest* **72**(1):404-408.

Mani S, Huang H, Sundarababu S, Liu W, Kalpana G, Smith AB and Horwitz SB (2005) Activation of the steroid and xenobiotic receptor (human pregnane X receptor) by nontaxane microtubule-stabilizing agents. *Clin Cancer Res* **11**(17):6359-6369.

Nardi A and Olesen SP (2008) BK channel modulators: a comprehensive overview. *Curr Med Chem* **15**(11):1126-1146.

Osmond RI, Sheehan A, Borowicz R, Barnett E, Harvey G, Turner C, Brown A, Crouch MF and Dyer AR (2005) GPCR screening via ERK 1/2: a novel platform for screening G protein-coupled receptors. *J Biomol Screen* **10**(7):730-737.

Power EC, Ganellin CR and Benton DC (2006) Partial structures of ketoconazole as modulators of the large conductance calcium-activated potassium channel (BK(Ca)). *Bioorg Med Chem Lett* **16**(4):887-890.

Raynal C, Pascussi JM, Leguelinel G, Breuker C, Kantar J, Lallemant B, Poujol S, Bonnans C, Joubert D, Hollande F, Lumbroso S, Brouillet JP and Evrard (2010) A Pregnane X Receptor (PXR) expression in colorectal cancer cells restricts irinotecan chemosensitivity through enhanced SN-38 glucuronidation. *Mol Cancer* **9**:46.

Rodriguez RJ and Acosta D, Jr. (1997) N-deacetyl ketoconazole-induced hepatotoxicity in a primary culture system of rat hepatocytes. *Toxicology* **117**(2-3):123-131.

Rodriguez RJ and Buckholz CJ (2003) Hepatotoxicity of ketoconazole in Sprague-Dawley rats: glutathione depletion, flavin-containing monooxygenases-mediated bioactivation and hepatic covalent binding. *Xenobiotica* **33**(4):429-441.

Rodriguez RJ, Proteau PJ, Marquez BL, Hetherington CL, Buckholz CJ and O'Connell KL (1999) Flavin-containing monooxygenase-mediated metabolism of N-deacetyl ketoconazole by rat hepatic microsomes. *Drug Metab Dispos* **27**(8):880-886.

Seglen PO (1976) Preparation of isolated rat liver cells. *Methods Cell Biol* **13**:29-83.

Takeshita A, Koibuchi N, Oka J, Taguchi M, Shishiba Y and Ozawa Y (2001) Bisphenol-A, an environmental estrogen, activates the human orphan nuclear receptor, steroid and xenobiotic receptor-mediated transcription. *Eur J Endocrinol* **145**(4):513-517.

Takeshita A, Taguchi M, Koibuchi N and Ozawa Y (2002) Putative role of the orphan nuclear receptor SXR (steroid and xenobiotic receptor) in the mechanism of CYP3A4 inhibition by xenobiotics. *J Biol Chem* **277**(36):32453-32458.

Wang H, Huang H, Li H, Teotico DG, Sinz M, Baker SD, Staudinger J, Kalpana G, Redinbo MR and Mani S (2007) Activated pregnenolone X-receptor is a target for ketoconazole and its analogs. *Clin Cancer Res* **13**(8):2488-2495.

Wang H, Li H, Moore LB, Johnson MD, Maglich JM, Goodwin B, Ittoop OR, Wisely B, Creech K, Parks DJ, Collins JL, Willson TM, Kalpana GV, Venkatesh M, Xie W, Cho SY, Roboz J, Redinbo M, Moore JT and Mani S (2008) The phytoestrogen coumestrol is a naturally occurring antagonist of the human pregnane X receptor. *Mol Endocrinol* **22**(4):838-857.

Wolf KK, Wood SG, Hunt JA, Walton-Strong BW, Yasuda K, Lan L, Duan SX, Hao Q, Wrighton SA, Jeffery EH, Evans RM, Szakacs JG, von Moltke LL, Greenblatt DJ, Court MH, Schuetz EG, Sinclair PR and Sinclair JF (2005) Role of the nuclear receptor pregnane X receptor in acetaminophen hepatotoxicity. *Drug Metab Dispos* **33**(12):1827-1836.

Yong WP, Ramirez J, Innocenti F and Ratain MJ (2005) Effects of ketoconazole on glucuronidation by UDP-glucuronosyltransferase enzymes. *Clin Cancer Res* **11**(18):6699-6704.

Yoshida K and Niwa T (2006) Quantitative structure-activity relationship studies on inhibition of HERG potassium channels. *J Chem Inf Model* **46**(3):1371-1378.

Molecular Pharmacology Fast Forward. Published on April 4, 2011 as DOI: 10.1124/mol.111.071787
This article has not been copyedited and formatted. The final version may differ from this version.

Footnotes

This work was supported by National Cancer Institute [CA12723101], Damon Runyon Foundation Clinical Investigator Award [CI 1502], and Phase I Program, Albert Einstein College of Medicine.

Disclosure Statement: The current ketoconazole analogs are under patent protection WO/2009/110955 (PCT/US2009/000524), by Albert Einstein College of Medicine, Bronx, NY 10461

Molecular Pharmacology Fast Forward. Published on April 4, 2011 as DOI: 10.1124/mol.111.071787
This article has not been copyedited and formatted. The final version may differ from this version.

Figure legends

Fig. 1. (A) Effect of azole compounds on The LanthaScreen TR-FRET PXR (SXR) competitive binding assay *in vitro*. Rifampicin was included as a positive control PXR ligand. (B&C) Effect of Cpd3 on hPXR and hPXR triple mutant (S247W/S208W/C284W) activity. Transactivation assays were performed using plasmids encoding (B) hPXR (C) triple mutant hPXR with respective reporters/ligands, as shown in the schematic diagram. Transfected cells were exposed to vehicle (0.2% DMSO), rifampicin 10 μM (Rif) with or without 25 μM Cpd 3. Columns, *mean*; bars, ±*SEM*, **P* <0.0048, ***P* <0.0280. (D) Effect of Cpd 3 on PXR target gene expression. RT-qPCR for human PXR and target genes (CYP3A4, MDR1 and UGT1A1) was carried out in LS174T cells exposed to rifampicin 10 μM (Rif) with or without 25 μM Cpd 3 or ketoconazole (KTZ) or vehicle (0.2% DMSO) for 48 h. Total RNA was isolated and subjected to RT-qPCR. β-actin served as an internal control. These experiments were performed two separate times each, assayed in triplicate. Columns, bars, ±*SD*.

Fig. 2. Effect of Cpd 3 on nuclear receptor target gene expression. Transactivation assays were performed using plasmids encoding **,** (A) mPXR, (B) LXRα, (C) FXR, (D) ERα , (E) PPARγ and (F) mCAR with respective reporters/ligands, as shown in the schematic diagrams. Transfected cells were exposed to vehicle (0.2% DMSO), pregnenolone-16alpha-carbonitrile 10 μM (PCN), T0901317 5 μM, chenodeoxycholic acid 50 μM (CDCA), Estradiol 20 μM, (E_2), and Rosiglitazone 10 μM (Rosi) with or without 10 μM Cpd 3 or 0.2% DMSO for 48 h. These experiments were performed three times in triplicate. Columns, bars, ±*SEM*. * $P < 0.001$.

Molecular Pharmacology Fast Forward. Published on April 4, 2011 as DOI: 10.1124/mol.111.071787
This article has not been copyedited and formatted. The final version may differ from this version.

Fig. 3. Effect of Cpd 3 on liver cells *in vivo*. Primary murine (A) and human (B) hepatocytes were exposed to ketoconazole (1-100 μM), Cpd 3 (1-100 μM), or vehicle (0.2% DMSO) for 48 h. Cells were then harvested and subjected to MTS assay (Materials and Methods). Experiments were repeated three separate times each in triplicate. Points, *mean*; bars, ±*SD*. (C) Mice were treated for 3 days with 0 to 600 mg/kg/day ketoconazole or Cpd 3 by oral administration; after animals were euthanized, liver tissues were stained with H&E. Representative sections from control and drug treated mice are shown. For orientation, the first (control) section denotes the Central vein (Cv). There is striking ballooning of hepatocytes in ketoconazole treated mice (liver concentration~ 45.9 μM). Drug concentrations in the liver, as analyzed using methods described in Materials and Methods, are illustrated in black. Hematoxylin & Eosin (H&E) staining, magnification 20x; the scale bar represents 50 μm. (D) Effect of ketoconazole and Cpd 3 on the expression of hepcidin-1 & 2 and SAA-1 & -3. Mice were treated for 3 days with 100 (n=3), 200 (n=3), 300 mg/kg/day (n=2) of Cpd 3 or 100 (n=3) mg/kg/day of ketoconazole, by oral administration. On day 3 after euthanasia, for each dose group, the livers were harvested and pooled, and total RNA was isolated from the pooled fraction and subjected to RT-qPCR, as described in Materials and Methods. The same RNA was assayed in three separate RT-qPCR experiments, each performed in duplicate. Columns, bars, ±*SEM*. Transaminase Enzymatic Assays were performed in pooled liver samples obtained from mice treated at 300 mg/kg/day for (E) AST and (F) ALT as described in Materials and Methods. The assay was repeated two times each, performed in triplicate. Columns, bars, ±*SEM*. * $P < 0.001$; ** $P < 0.001$

Fig. 4. The effects of Cpd 3 on PXR induced chemoresistance *in vitro and* anesthetic (tribromoethanolamine) metabolism *in vivo*. (A&B) Cell cytotoxicity from the anticancer drug

Molecular Pharmacology Fast Forward. Published on April 4, 2011 as DOI: 10.1124/mol.111.071787
This article has not been copyedited and formatted. The final version may differ from this version.

SN-38 in LS174T (transduced with scrambled or PXR shRNA) colon cancer cells pretreated with rifampicin (Rif) or vehicle (0.2% DMSO) and/or Cpd 3. LS174T cells were pretreated (for 24 h) with 15 μM Rif or vehicle and/or 10 μM Cpd 3 and then exposed to SN-38 (0.0-50 μM) for another 24 h. Each experiment was performed three times in triplicate. Points or columns, *mean*; bars, ±*SD*. # $P < 0.0001$. Cpd 3 modulates anesthetic (tribromoethanolamine) metabolism *in vivo*. Loss of righting reflex (LORR) duration was performed as described in Materials and Methods (Animal Studies) to determine the effect of Cpd 3 in (C) $pxr^{+/+}$ (D) *hPXR (*E) $pxr^{-/-}$ mice. Columns, bars, ±*SEM*. * $P < 0.001$, ** $P < 0.05$

Fig. 5. Determination of ALT activities in serum of PXR wild type mice following PCN, APAP and Cpd3 combinatorial treatment groups. PXR wild type mice (n=8/groups) were pretreated with corn oil (vehicle) or Cpd 3 on day –1 prior to PCN dosing and continued through acetaminophen dosing for a total of 4 days. Blood was collected and serum was separated as described in the Materials and Methods section. ALT levels were measured according to the manufacturer's instructions. Columns, bars, ±*SEM*. * $P < 0.05$, ** $P < 0.05$

Fig. 6. hERG tail current density averages obtained by measuring the hERG tail peak amplitude at -7 mV in baseline conditions and in the presence of 5, 10, 20 and 50 μM Ketoconazole (Table 2) or Cpd3 (Table 3). A: Representative recordings of activating and inactivating hERG currents in baseline conditions (black), and following exposure of the cells to 50 μM ketoconazole, or 50 μM Cpd3 (red). B: Current density was measured from 7 cells, averaged, normalized against baseline current density, and corrected for time and solvent effects. KTZ IC50 is 18 μM Cpd3 is not available. Statistical comparisons between post-drug exposure and baseline current density

Molecular Pharmacology Fast Forward. Published on April 4, 2011 as DOI: 10.1124/mol.111.071787
This article has not been copyedited and formatted. The final version may differ from this version.

levels were made using repeat paired Student's t-tests: Differences were considered significant when $P \leq 0.05$.

Fig. 7. Effects of Ketoconazole and Cpd3 on on the activation phase of the hERG current. Voltage pulse protocol used. Pulse 1 was used to determine channel activation kinetics and steady-state current-voltage relationship while pulse 2 was used to determine the channel inactivation and current rectification. B, C: I-V relationship for current measured at the end of depolarizing step from Pulse #1 when exposed to Ketoconazole (B) and to Cpd3 (C). (D) Changes in hERG activation time constant induced by Ketoconazole and Cpd3: activation constants were corrected for the effect of DMSO on activation kinetics.

Molecular Pharmacology Fast Forward. Published on April 4, 2011 as DOI: 10.1124/mol.111.071787
This article has not been copyedited and formatted. The final version may differ from this version.

Table 1. Cpd 3 concentrations in mouse and human tumor xenograft tissues

Samples	Treatment group	Concentration (μM)
Plasma	Cpd 3	28.0± 3.5
	Rifampicin/Cpd 3	33.31 ± 1.69
Liver	Cpd 3	23.45 ± 1.55
	Rifampicin/Cpd 3	23.1± 4.4
Tumor (LS174T xenografts)	Cpd 3	24.5 ± 2.1
	Rifampicin/Cpd 3	23.475 ± 3.325

Table 1. Six- to eight-week-old C57BL/6 female and SCID/NOD mice xenografted with LS174T cells (group average flank tumor volume ~0.45 mm^3) were injected with rifampicin (ip 50 mg/kg/day) and/or orally gavaged Cpd 3 (300 mg/kg/day) for 4 days. All tissues were harvested on day 4 for assessment of Cpd 3 concentrations, as described in Materials and Methods.

Molecular Pharmacology Fast Forward. Published on April 4, 2011 as DOI: 10.1124/mol.111.071787
This article has not been copyedited and formatted. The final version may differ from this version.

Table 2. Normalized hERG tail current values at -7 mV when exposed to Ketoconazole and corrected for the DMSO effect

Conditions	Corrected Normalized Current Density	SEM	p value	(n=)
Baseline	1.000	0.000	N/A	7
Ketoconazole 5 µM	0.706	0.086	0.0064	7
Ketoconazole 10 µM	0.608	0.084	0.0007	7
Ketoconazole 20 µM	0.474	0.078	0.0001	7
Ketoconazole 50 µM	0.302	0.038	0.0000	7

Table 3. Normalized hERG tail current values at -7 mV when exposed to Cpd3 and corrected for the DMSO effect

Conditions	Corrected Normalized Current Density	SEM	p value	(n=)
Baseline	1.000	0.000	N/A	7
Cpd3 5 µM	0.822	0.067	0.0126	7
Cpd3 10 µM	0.732	0.072	0.0013	7
Cpd3 20 µM	0.644	0.125	0.0058	7
Cpd3 50 µM	0.576	0.123	0.0026	7

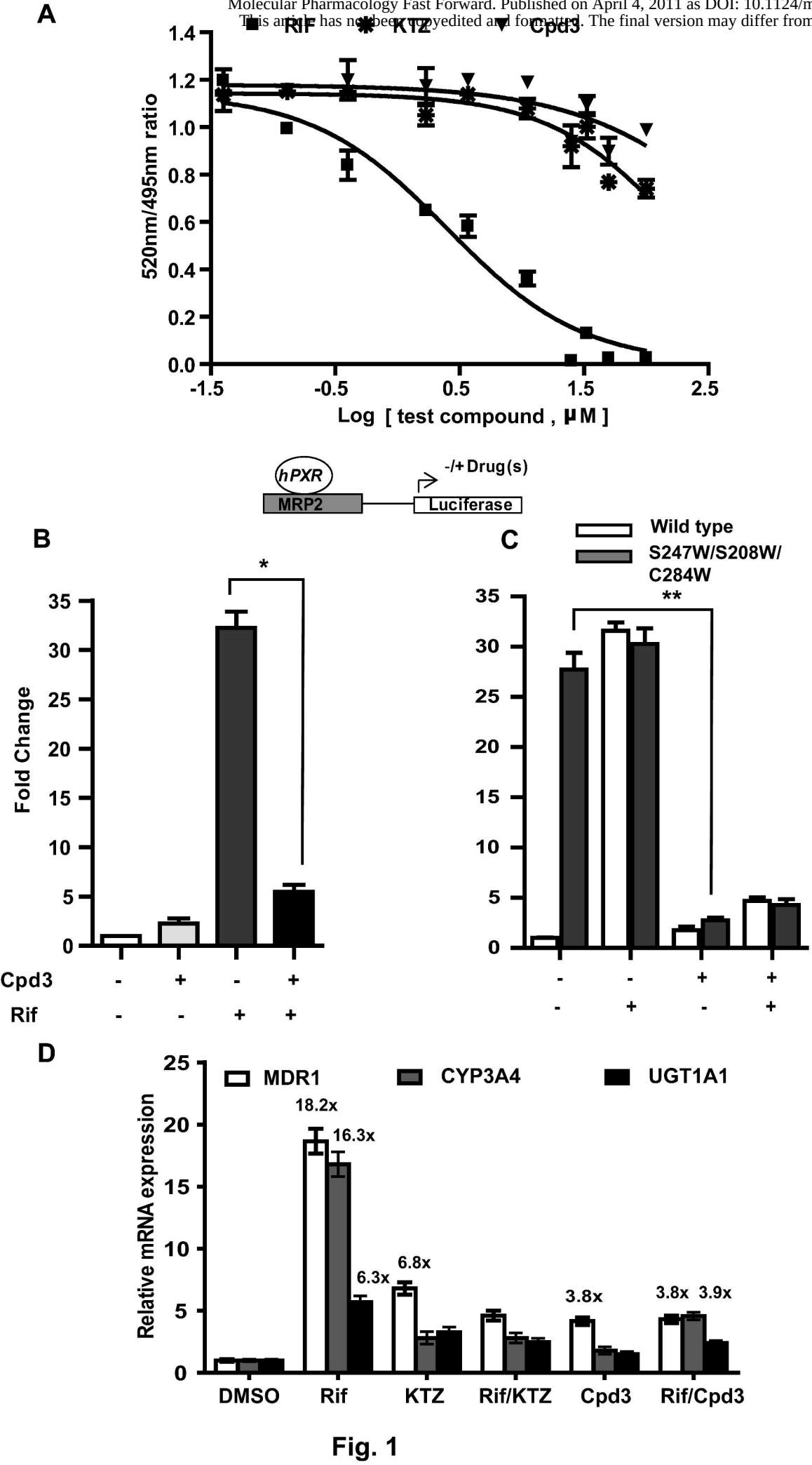

Fig. 1

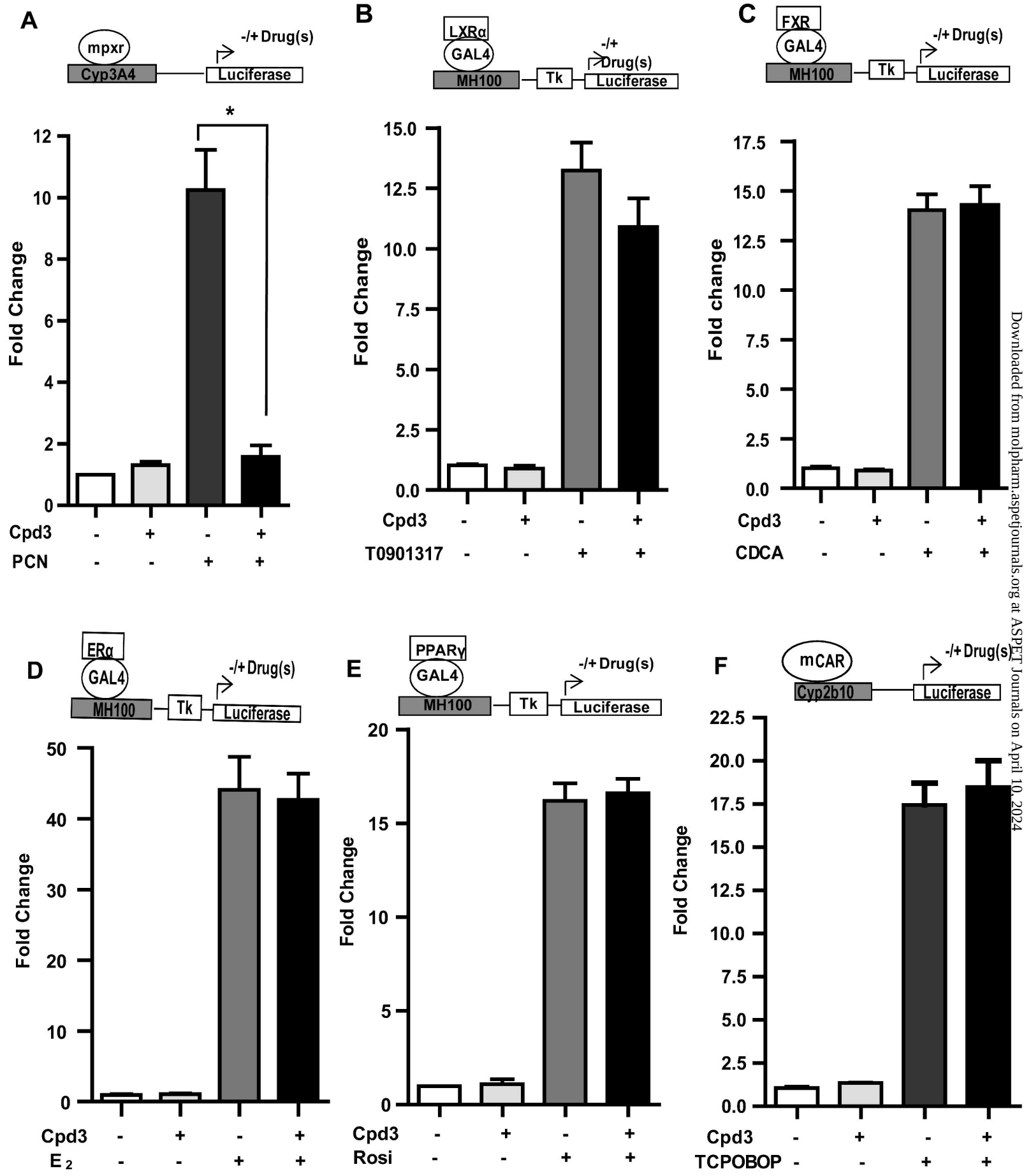

Fig. 2

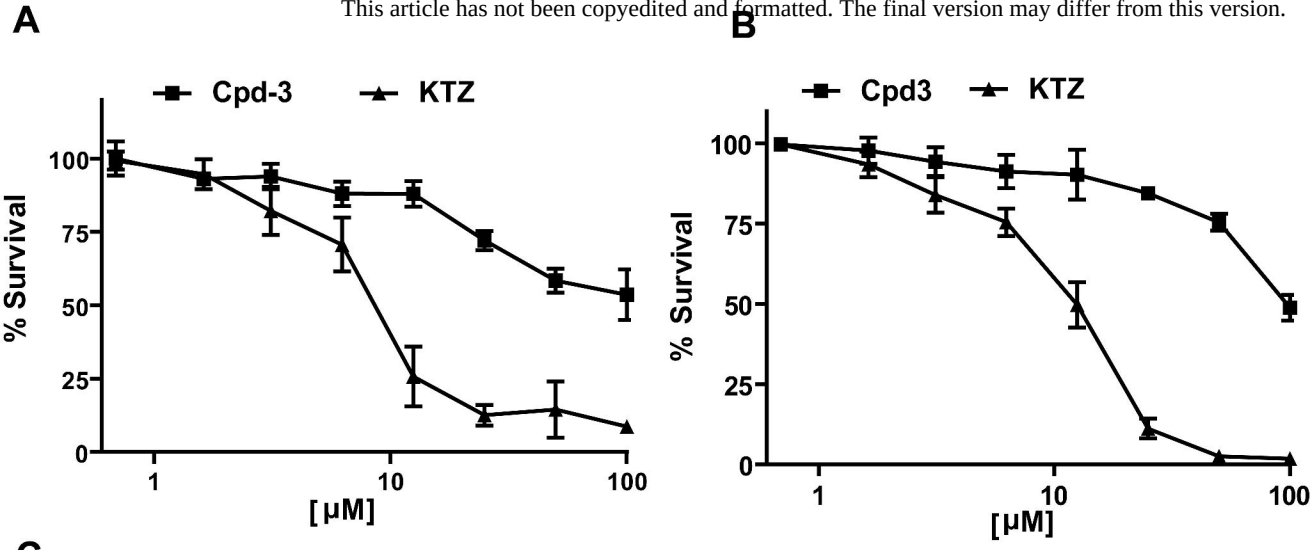

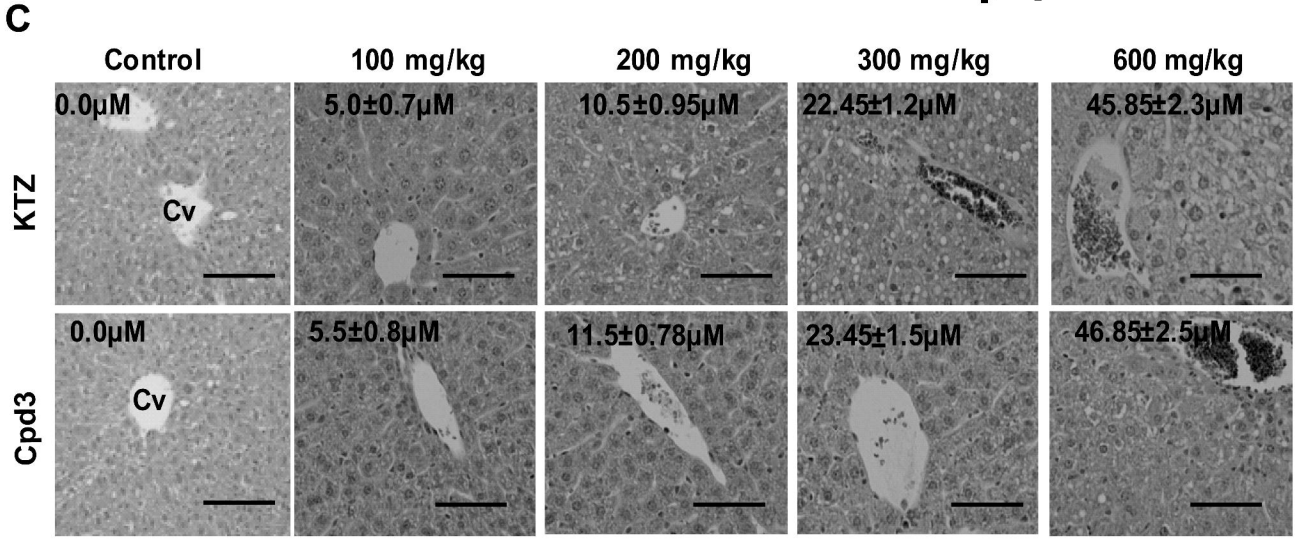

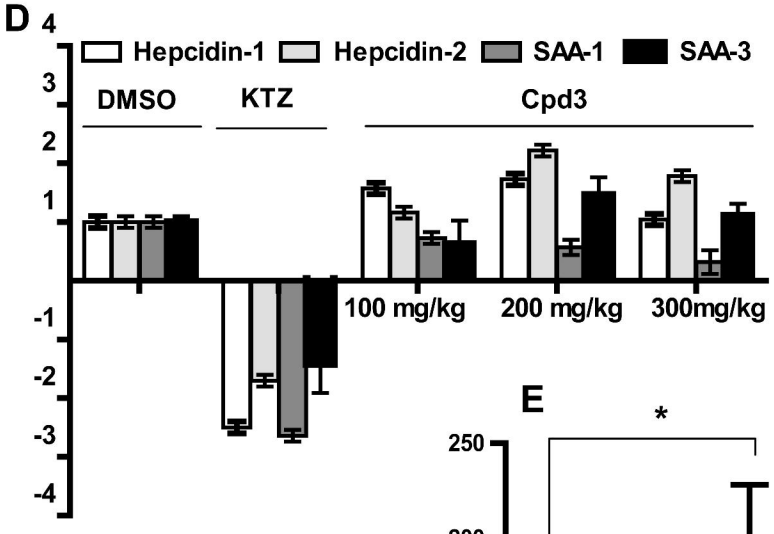

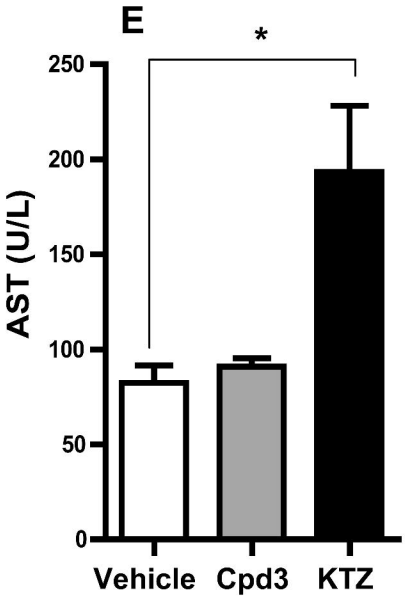

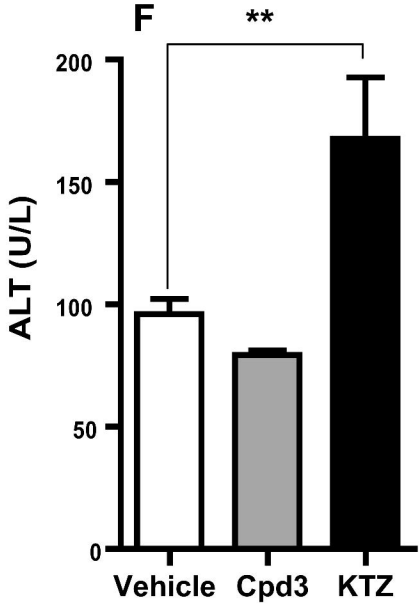

Fig. 3

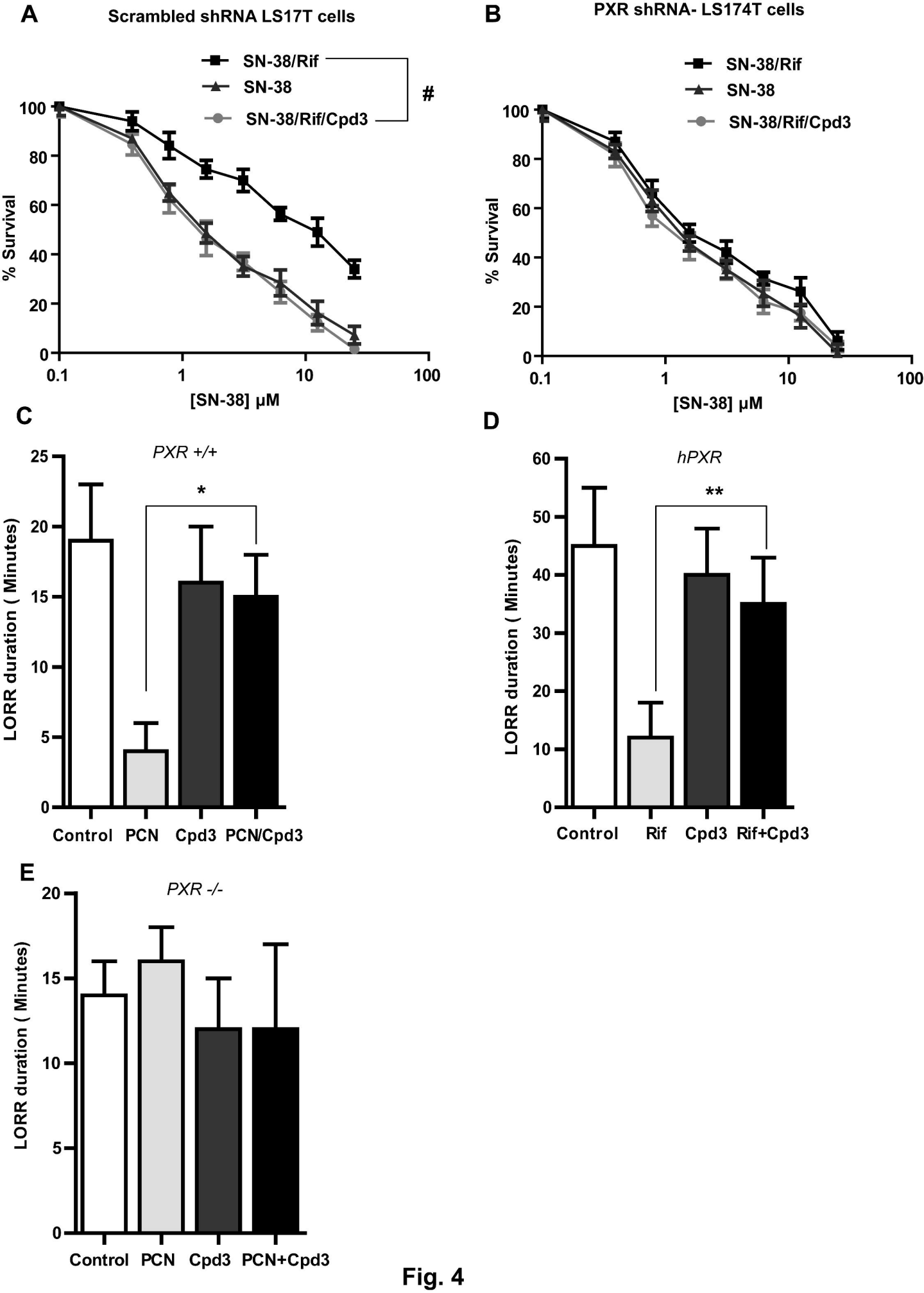
A
Scrambled shRNA LS17T cells
SN-38/Rif
SN-38
SN-38/Rif/Cpd3
#
% Survival
[SN-38] µM
B
PXR shRNA- LS174T cells
SN-38/Rif
SN-38
SN-38/Rif/Cpd3
% Survival
[SN-38] µM
C
PXR +/+
*
LORR duration (Minutes)
Control
PCN
Cpd3
PCN/Cpd3
D
hPXR
**
LORR duration (Minutes)
Control
Rif
Cpd3
Rif+Cpd3
E
PXR -/-
LORR duration (Minutes)
Control
PCN
Cpd3
PCN+Cpd3

Fig. 4

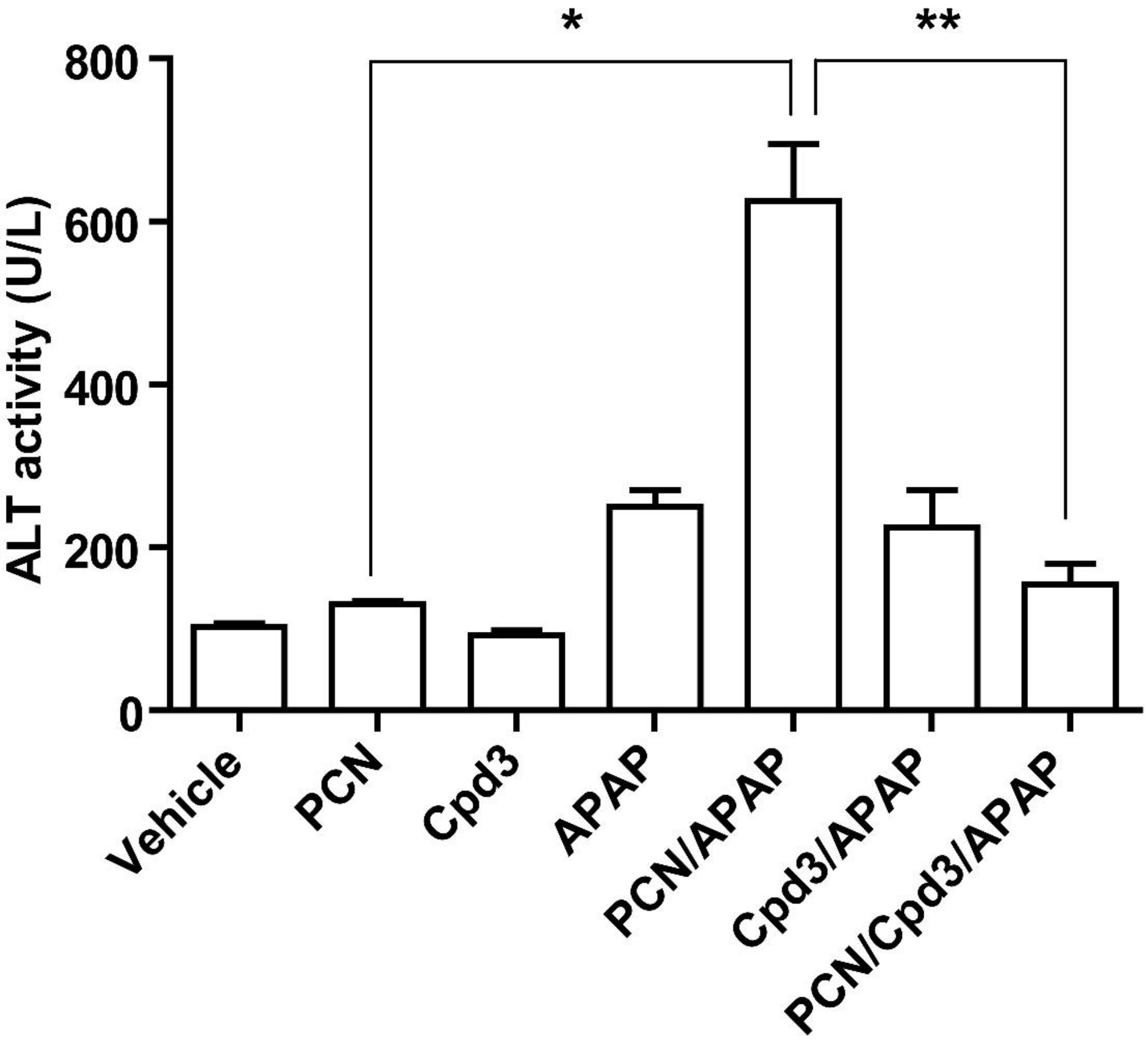
*
**
800
600
400
200
0
ALT activity (U/L)
Vehicle
PCN
Cpd3
APAP
PCN/APAP
Cpd3/APAP
PCN/Cpd3/APAP

Fig. 5

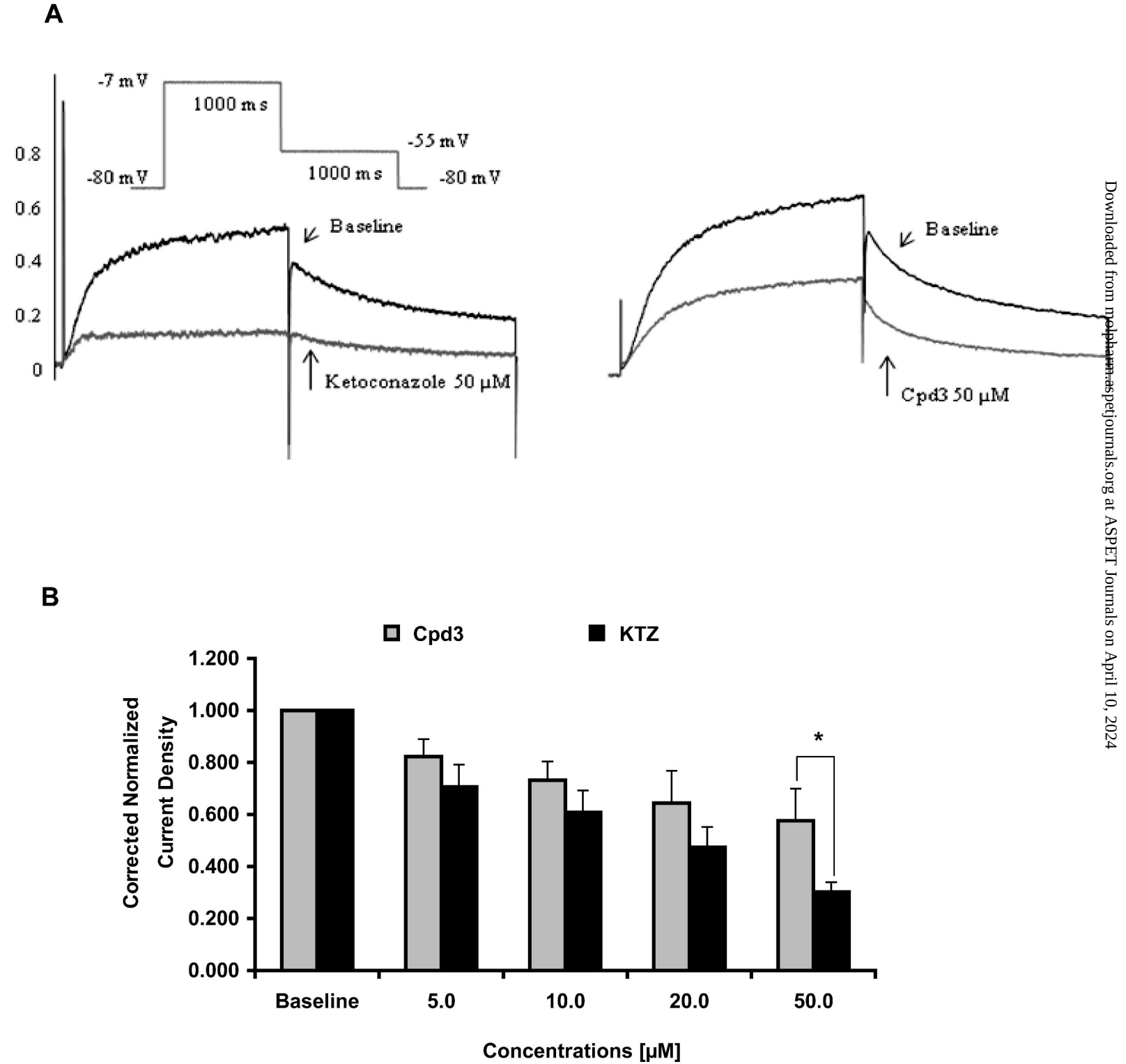

Fig. 6

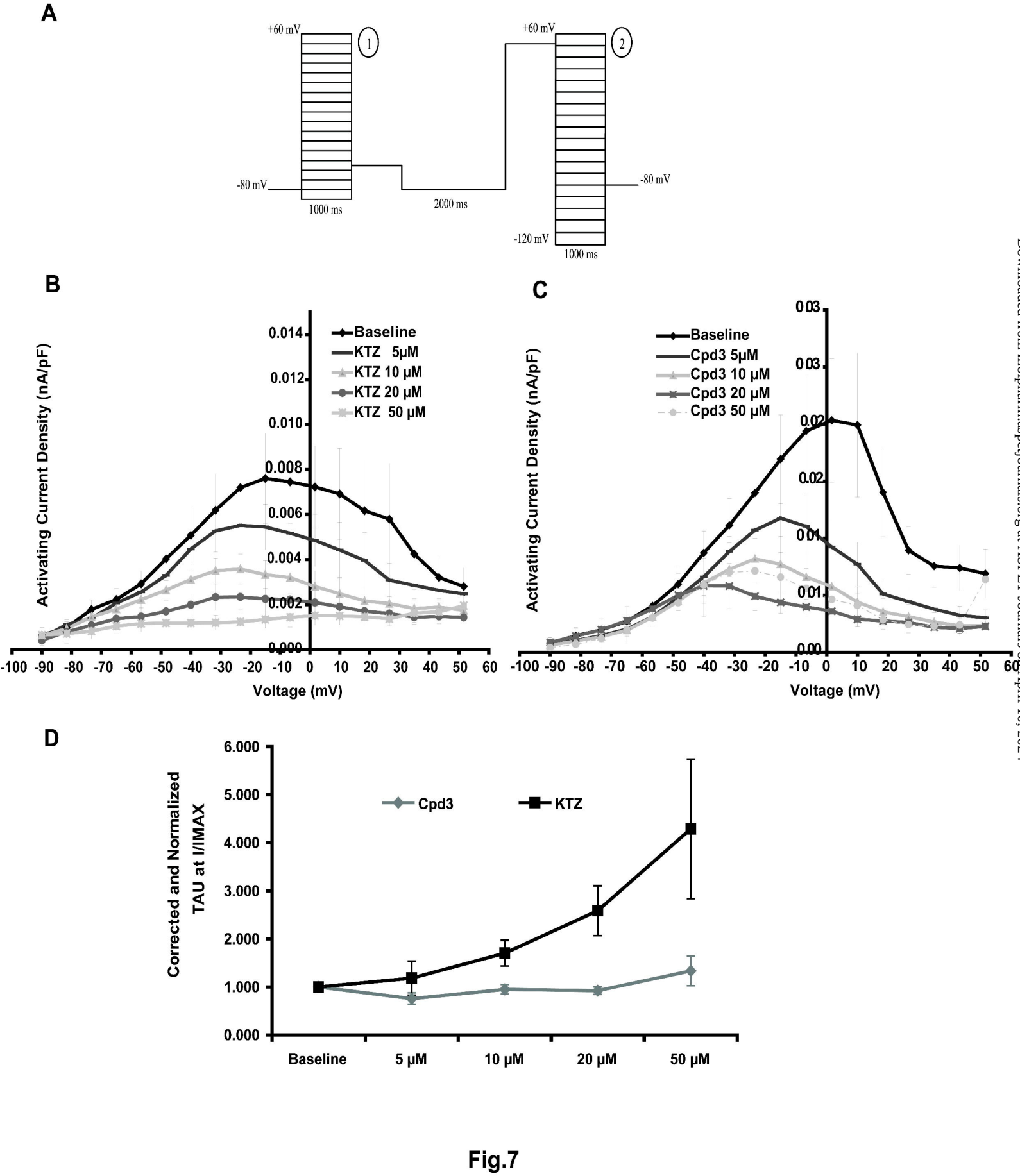
A
+60 mV
1
+60 mV
2
-80 mV
-80 mV
1000 ms
2000 ms
-120 mV
1000 ms
B
Activating Current Density (nA/pF)
Baseline
KTZ 5μM
KTZ 10 μM
KTZ 20 μM
KTZ 50 μM
Voltage (mV)
C
Activating Current Density (nA/pF)
Baseline
Cpd3 5μM
Cpd3 10 μM
Cpd3 20 μM
Cpd3 50 μM
Voltage (mV)
D
Corrected and Normalized TAU at I/IMAX
Cpd3
KTZ
Baseline
5 μM
10 μM
20 μM
50 μM

Fig.7